Zwischenbericht

Förderprogramm:	**Virtuelle Institute**
Impulsfonds-Projektnummer:	VH-VI-403
Projekttitel:	In-Situ Nano-Imaging of Biological and Chemical Processes
Sprecher des Virtuellen Instituts	Christian Schroer
Berichtszeitraum (Förderungszeitraum)	01.09.2011 – 31.12.2011

Sachbericht

a) Fortschritt des im Antrag beschriebenen Arbeitsprogramms

The proposal forsees contributions of the VI to a variety of scientific fields. In the first four months, the activities in the different scientific areas were started. In particular, the following first results were obtained:

Heterogeneous Catalysis & Sintering

In catalysis it is very important to push chemical imaging from millimeters and micrometers to the submicrometer scale. As a joint effort of the Grunwaldt and Schroer group, different approaches have been tackled including full-field hard X-ray microscopy, scanning X-ray microscopy and ptychography. The schematic is shown in Figure 1 for exhaust gas catalysis, where the active catalyst layer is deposited as “washcoat” on a cordierite honeycomb.

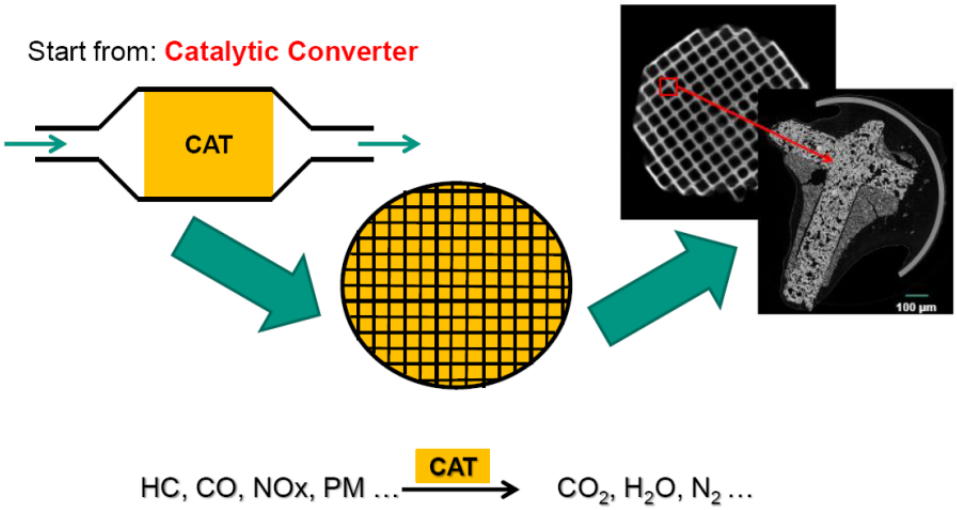

Figure 1: Principle for catalyst understanding – from the macro to the microscale (the honeycomb structure on the top right was imaged in tomography with a lab source; the structural details were taken by full-field X-ray microscopy (see Figure 2).

In order to learn more about the washcoat structure, full-field X-ray microscopy was performed. Figure 2 shows the tomographic reconstruction of a single slice out of more than 1700 other slices as an example. The cordierite, the cross-like structure in Fig. 2, reveals its high porosity and shows hardly any deposition of the washcoat inside the porous structure. The washcoat layer contains cracks and local variations visible in the reconstruction. It

remains well separated from the cordierite structure and is easily distinguished by eye due to the different density and texture.
Full-field tomography yields a spatial resolution in three dimensions of slightly below 1 µm, and a full-field tomographic reconstruction is shown in Figure 2. This tomogram allows a detailed study of the pore structure, which is a valuable input for simulation of the heat and mass transport in the porous layers and the honeycomb in general.

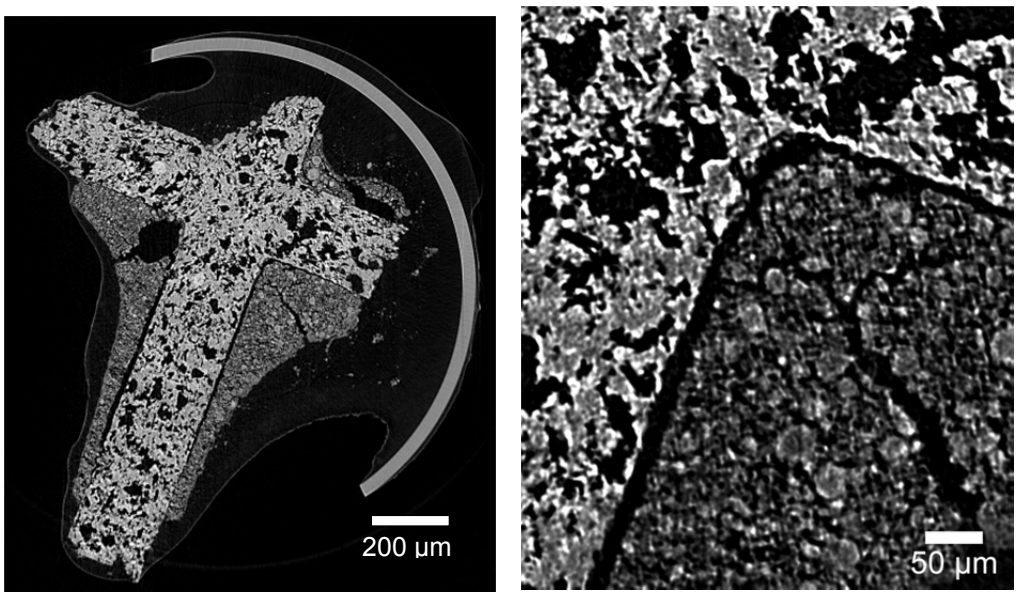

Figure 2: Left: Slice of a tomographic reconstruction with sub-µm resolution recorded at beamline P06 of PETRA III of a cross-like fraction of the ceramic support which is covered by a layer of washcoat containing the catalytically active species. Right: Lower right corner of the cross on the left shown in 100% zoom. Single bright spots in the washcoat become visible, suggesting Pt clusters.

To investigate the activity of individual catalyst particles in operando, it is planned to combine absorption spectroscopy with ptychographic microscopy to image the interior of a catalytic microreactor. While the catalytic microreactor will be designed and built in 2012, a test experiment was carried out to verify the feasibility of chemical imaging of individual metallic nanoparticles with spectroscopic contrast.

For this purpose, a series of ptychograms of a test sample made of gold particles was recorded at energies around the gold L_3 edge. Figure 3a) shows an SEM image of the gold particles (size of individual particles approx. 80 nm) on a silicon-nitride membrane. A ring made of platinum is deposited around the particles as a reference for the spectroscopy and as a fiducial marker. (The sample was prepared and precharacterized in collaboration with C. Damsgaard from DTU in Copenhagen, Denmark.) In Fig. 3b) a ptychographic reconstruction of the sample is shown for an energy below the gold L_3 edge (E = 11.900 keV). It was recorded with the hard x-ray scanning microscope at beamline P06 at PETRA III at DESY in Hamburg. The gold particles are clearly resolved. In Fig. 3c) the phase shifts in a region of interest on the gold particles and on the platinum ring are shown as a function of x-ray energy. The reduction of the (negative) phase shift as a result of anomalous dispersion in the gold particles is clearly visible [red curve in Fig. 3c)]. The smallest (negative) phase shift coincides with the inflection point of the absorption spectrum of a metallic gold foil [red dashed curve in Fig. 3c)], showing that the gold in the nanoparticles is in a metallic state. For comparison, the platinum spectrum is flat as expected around the L_3 edge of gold [blue curve in Fig. 3c)].

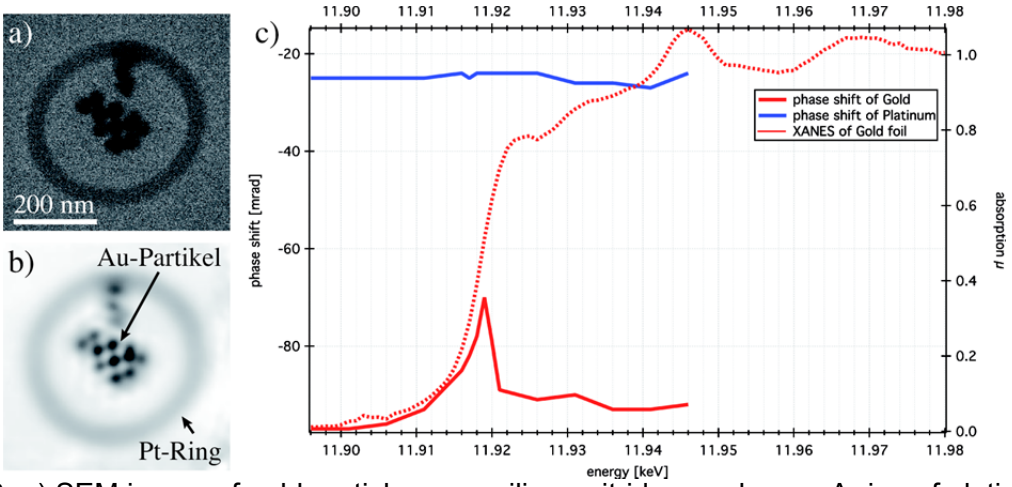

Figure 3: a) SEM image of gold particles on a silicon-nitride membrane. A ring of platinum was deposited around the cluster of particles as a fiducial marker. b) Ptychogram (phase shift) of the sample at an x-ray energy of E = 11.900 keV. c) Phase shift as a function of energy for a region of interest (ROI) on the gold particles (red curve) and on the platinum ring (blue curve). For comparison the near edge spectrum of a gold foil is shown as reference (red dashed curve).

With the help of ptychography it is thus possible to record high-resolution images of small objects with chemical near-edge contrast. A spatial resolution clearly below 100 nm was reached. In a next step, we will try to ignite a catalytic reaction over nanoparticles in a microreactor that is currently developed and image the chemical state and thus the catalytic activity of the particles with near-edge spectroscopic ptychography.

Coherent Imaging of Biological Cells and Tissues at P10/GINIX

The optics of the nanofocus setup GINIX (Göttingen Instrument for Nano-Imaging with X-rays) has been significantly augmented by a setting, which allows for a fully coherent KB beam. Closing slits in front of the KB and using pinholes as filters, full coherence is achieved as well as an aberration corrected wavefront. First proof-of-concept experiments in ptychography and full-field propagation imaging have shown the unique potential of this setting for ptychography in a high-flux setting, as well as for fast tomography (full-field mode by moving the sample out of focus). After this improvement, the limits (in speed) are now given by detector read-out, which will also undergo further improvements. High spatial resolution in nano-focusing has been reached by two schemes: (i) a crossed waveguide arrangement with 10 nm focusing in two directions [2], and (ii) a combination of KB and multilayer Laue lens [3]. Concerning sample environment, a sample cell for imaging of membranes in solution has been tested at P10, and the cryo-jet system has been successfully installed. The following applications in biological imaging have been carried out: tomography of fixated optical and sciatic nerves, coherent imaging of fixated and of live nematodes (C. elegans), coherent imaging of tissue slices from rat and mouse central nervous system, freeze dried and frozen hydrated cells (amoeba *D. discoideum*, bacterial cells of *D. radiodurans.* A collaborative experiment on structure analysis of melanosomes was carried out by the Rosenhahn and the Salditt groups at P10.

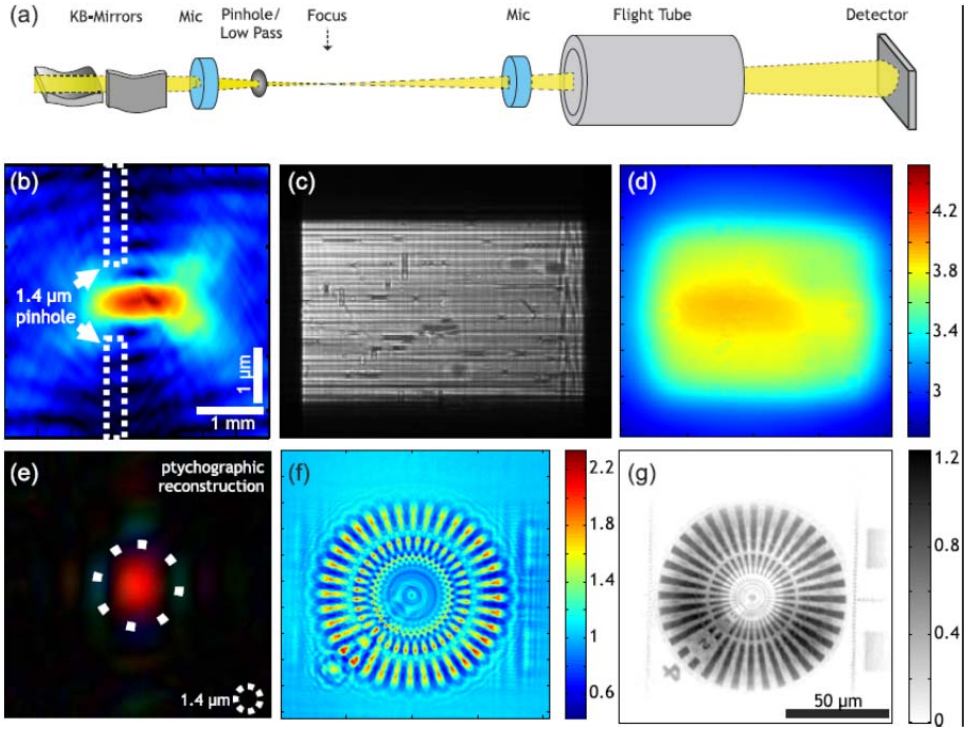

Figure 4: (a) Schematic of the setup for coherent KB imaging, (b) ptychographically reconstructed KB focusing along the optical axis showing residual intensity in the tails of the focus. The position of the cleaning pinhole is indicated. (c) Typical KB far-field at conditions of partial coherence showing high frequency stripes due to figure errors of the mirrors and wavefront aberrations inhibiting propagation imaging. (d) ``Clean'' KB far-field after filtering with a pinhole in the focal plane, and after closing the upstream slits. (e) Ptychographic probe retrieval will be used for further control of the wavefronts, here showing the illumination in the focal plane corresponding to the far field shown in (d). (f) Recorded (magnified) hologram of a test structure after dividing by the empty beam, and (g) corresponding reconstruction (64nm pixel size and 120µm x 120µm field of view. Note that the entire Siemens star is recorded in a single shot. No artifacts are visible, enabling quantitative phase reconstructions in full field mode well suited for fast tomography (Bartel el. al, unpublished results).

Nanodiffraction on protein structures in cells

In a collaboration between the groups of Tim Salditt and Sarah Köster, experiments at P10/GINIX were performed on the inner structure of proteins in cells. The biological systems we looked at were (i) keratin bundles in epithelial cells and (ii) actin bundles in stereocilia of hair cells. Both systems were chosen for their known, very distinct structure built up of individual biopolymers. The keratin bundles in epithelial cells contribute considerably to cell mechanics, while actin in stereocilia is essential for hearing and sense of balance. In Figure 5 an example can is shown for a keratin network in the cells. In the region-of-interest dark field representation the network can clearly be distinguished from the background regions.

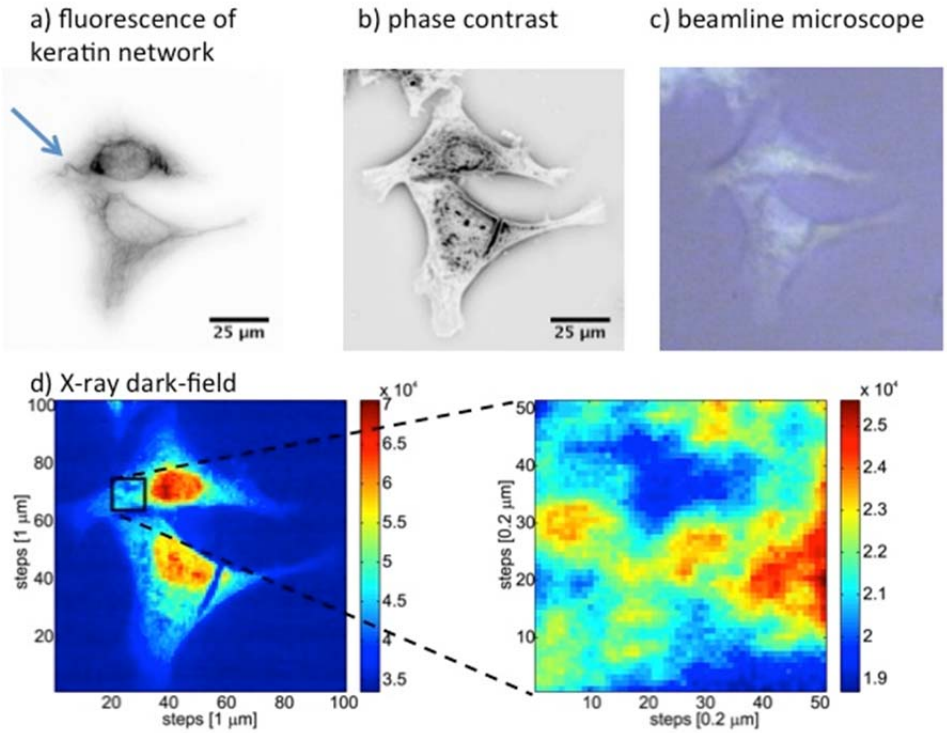

Figure 5: Nano-diffraction on a keratin network in a cell. a) Visible light fluorescence micrograph which shows the network (inverted, dark is the protein). b) Phase contrast image after freeze drying the sample. c) Image taken by the beamline microscope. d) X-ray dark field contrast of the whole region and of a smaller region of interest.

Coherent Imaging of cryogenic biological samples with HORST

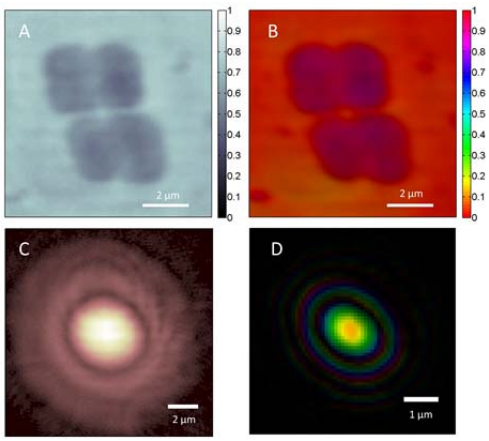

Figure 6: Reconstruction of ptychography scans of frozen hydrated *Deinococcus radiodurans,* recorded with a 2 µm pinhole. (A) shows the absorption contrast and (B) the phase contrast. (C) shows the illuminating wavefront in the sample plane and (D) the wavefront backpropagated into the pinhole plane. A photon energy of 517 eV has been used.

The HORST chamber has been equipped with a cryogenic sample environment in order to investigate frozen hydrated biological samples. Along with establishing the cryogenic stage, preparation of the samples has been optimized and the workflow of culturing, plunge freezing, transfer and coherent imaging has been optimized. Using soft X-rays provided by UE49/2 at BESSY, first Ptychographic images of frozen diatoms and bacteria were recorded.

Absorption scans along the oxygen K edge reveal that the thickness of the ice layer after vitrification is in the order of 1.6 µm. In a collaboration of the Salditt and the Rosenhahn group, frozen hydrated *Deinococcus radiodurans* were imaged by Ptychography. The reconstructions are shown in Figure 6. (A) shows the obtained absorption contrast images and (B) the phase contrast images. In can be seen that also in the frozen hydrated stage, both, absorption and phase contrast contribute to image formation when soft X-rays are used. (C) and (D) show the retrieved probe functions in the sample and in the pinhole plane, respectively. Besides *D. radiodurans*, the diatom *Navicula perminuta*, melanosomes and fibroblast cells were investigated.

Three-dimensional structure of a single colloidal crystal grain studied by coherent x-ray diffraction

The group of Ivan Vartaniants has performed a coherent x-ray diffraction experiment on an isolated colloidal crystal grain at the coherence beamline P10 at PETRA III [13]. Using azimuthal rotation scans the three-dimensional (3D) scattered intensity from the sample in the far field was measured [see Fig. 7]. It includes several Bragg peaks as well as the coherent interference around these peaks. The analysis of the scattered intensity reveals the presence of plane defects in a single grain of the colloidal sample. We confirm these findings by model simulations. In these simulations we also analyze the experimental conditions required to phase the 3D diffraction pattern from a single colloidal grain [see Fig. 8]. This approach has the potential to produce a high resolution image of the sample revealing its inner structure, with possible structural defects.

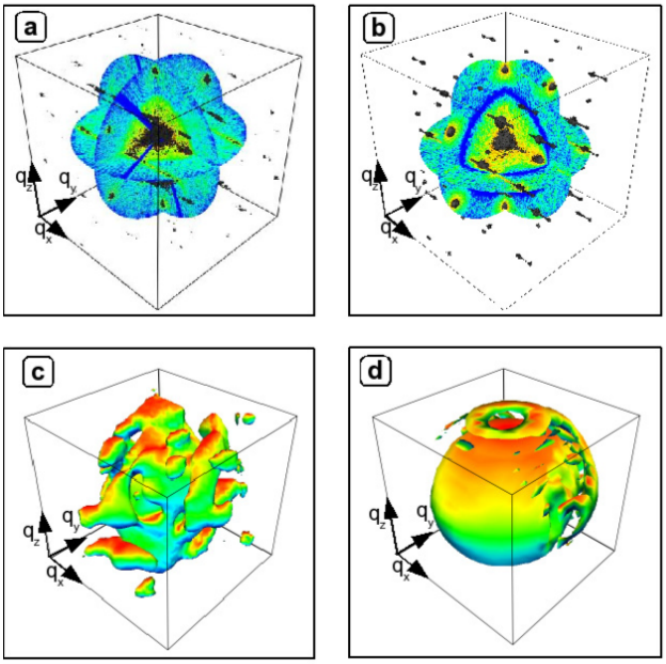

Figure 7: (a, c) Experiment and (b, d) simulations. (a, b) A 3D representation of the measured (a) and simulated (b) scattered intensity showing three orthogonal planes and an isosurface. The length of the arrows corresponds to 30 μm^{-1}. (c, d) An isosurface of measured (c) and simulated (d) scattered intensities around a 220 Bragg peak. The length of the arrows corresponds to 2.5 μm^{-1}.

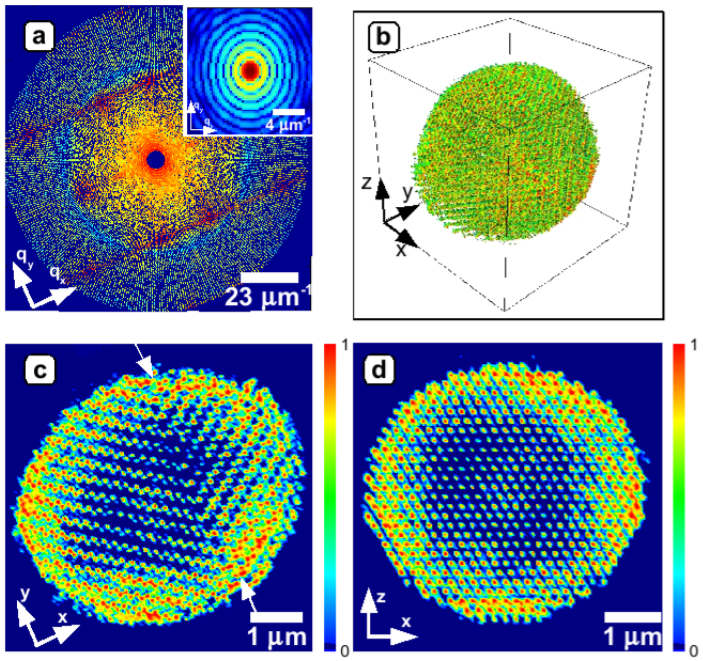

Figure 8: (a) The (q_x - q_y) cut in reciprocal space obtained from simulated 2D diffraction patterns with one-degree increment. The missing region covers the central speckle and two first fringes. (inset) A slice through 3D scattered intensity around a 220 Bragg peak. (b) An isosurface of the reconstructed object, the length of the arrows corresponds to 2 µm. (c, d) Two orthogonal cuts through the reconstructed object. The arrows in (c) point to the defect in the colloidal grain.

Dynamics of colloidal crystals studied by pump-probe experiments at FLASH

The group of Ivan Vartaniants in collaboration with the groups of Tim Salditt and Axel Rosenhahn performed a time-resolved infrared (IR) pump and extreme-ultraviolet (XUV) probe diffraction experiment [unpublished] to investigate ultrafast structural dynamics in colloidal crystals with picosecond resolution. The experiment was performed at the FLASH facility at DESY with a fundamental wavelength of 8 nm [see Fig. 9]. In our experiment, the temporal changes of Bragg peaks were analyzed and their frequency components were calculated using Fourier analysis. Periodic modulations in the colloidal crystal were localized at a frequency of about 4–5 GHz. Based on the Lamb theory, theoretical calculations of vibrations of the isotropic elastic polystyrene spheres of 400 nm reveal a 5.07 GHz eigenfrequency of the ground (breathing) mode.

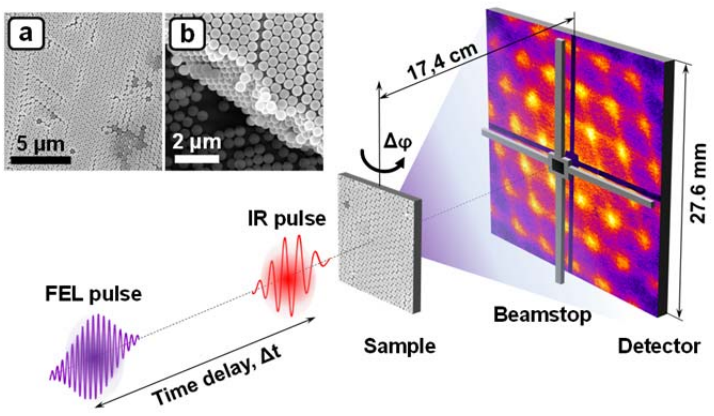

Figure 9: Schematic view of the pump-probe experiment showing the infrared pump (IR pulse) and the extreme-ultraviolet probe (FEL pulse) separated by a time delay Δt, the

sample, and the detector which is protected by the beamstop. Insets (a) and (b) show SEM images of the colloidal crystal film used in the experiment. The eleven layers of polystyrene spheres composing the colloidal crystal are visible in the inset (b).

Spatial and temporal coherence properties of single free-electron laser pulses

The group of Ivan Vartaniants in collaboration with the groups of Axel Rosenhahn and Wilfried Wurth performed the experimental characterization of the spatial and temporal coherence properties of the free-electron laser in Hamburg (FLASH) at a wavelength of 7.9 nm [unpublished]. Double pinhole diffraction patterns of single femtosecond pulses focused to a size of about 10 x 10 μm^2 (FWHM) were measured [see Fig. 10a]. A transverse coherence length of 7 µm in the horizontal and 8 µm in the vertical direction was determined from the most coherent pulses. Using a split and delay line [see Fig. 10b] the temporal coherence time of the pulses produced in the same operation regime of FLASH was measured to be 1.7 fs.

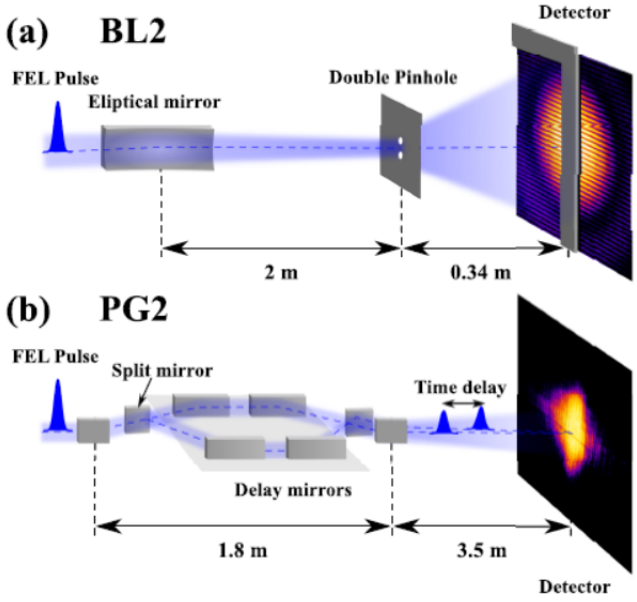

Figure 10: A sketch of the experiment. a) Young's double pinhole experiment to characterize the spatial coherence of the incident beam at the BL2 beamline. b) The split and delay unit at the PG2 beamline splits the incoming beam into two beams. Both beams are recombined in space on the detector. Due to the geometry of the setup both beams overlap with a small angle.

b) Erreichte Meilensteine

In the short reporting period since kick off, there were no milestones to be reached.

c) Einhaltung des Finanzierungs- und Zeitplans

The project started as planned. There are no deviations from the financial and time schedule.

d) Publikationen, Vorträge, Preise etc. bitte gegebenenfalls als Anhang beifügen

Meetings:

The Kick-off meeting was held in Göttingen on Oct. 4, 2011 (full day). All participating groups presented their current activities and the common future activities were discussed.

Oral Presentations:

Jan-Dierk Grunwaldt, "Probing Catalysts in Action: Time and spatially resolved information using X-ray absorption spectroscopy", EUROPACAT, (1.9.2011)(keynote lecture)□□

Jan-Dierk Grunwaldt, "How to grab dynamics in catalysis – shining light on catalysts", Workshop: From Detailed Microkinetics to the Reactor, Munich, (6.9.2011) (invited)□□

Georg Hofmann and Jan-Dierk Grunwaldt, "Imaging in Catalysis Research: Towards tomographic and dynamic studies using synchrotron radiation", Lund, (24-26.11.2011)(invited)

S. Köster “X-Ray studies of biomatter in microfluidic environments”, Argonne National Lab, Advanced Light Source, USA (22.9.2011)(invited)

S. Köster “Microfluidic approaches to physical properties of bio-systems”, SFB 647 Symposium, LMU Munich, Germany (7.10.2011)(invited)

S. Köster “Biophysics in microflow”, Biozentrum Basel, Switzerland (22.11.2011)(invited)

S. Köster “Polymers in microchannels”, Institut Curie, Paris, France (14.12.2011)(invited)

T. Salditt “X-ray nano-focusing with pre-shaped mirrors and waveguides”, FOURTH INTERNATIONAL SYMPOSIUM on Atomically Controlled Fabrication Technology, Osaka, Japan (10/31/2011-11/02/2011)(invited)

C. Schroer, “X-Ray Microscopy with Coherent Radiation,” ICXOM21, Indaiatuba, Brazil (09/08/2011)(plenary talk)

Publications:

[1] C. G. Schroer, G. Falkenberg, C. David, Photon Science 2011, “Hard X-ray nanoprobe at PETRA III”, 100-101 (DESY, 2011).

[2] S.P. Krueger, H. Neubauer, M. Bartels, S. Kalbfleisch, K. Giewekemeyer, P. J. Wilbrandt, M. Sprung and T. Salditt , Sub-10 nm beam confinement by X-ray waveguides: design, fabrication and characterization of optical properties, J. Synchrotron Rad. (2012). 19, 227-236

[3] A. Ruhlandt, T. Liese, V. Radisch, S. P. Kruger, M. Osterhoff, K. Giewekemeyer, H. U. Krebs, and T. Salditt , A combined Kirkpatrick-Baez mirror and multilayer lens for sub-10 nm x-ray focusing , AIP ADVANCES 2, 012175 (2012) .

[4] A. Beerlink, S. Thutupalli, M. Mell, M. Bartels, P. Cloetens, S. Herminghaus and T. Salditt , X-Ray propagation imaging of a lipid bilayer in solution , Soft Matter, 8, 4595-4601 (2012)

[5] T. Gorniak, R. Heine, A. P. Mancuso, F. Staier, C. Christophis, M. E. Pettitt, A. Sakdinawat, R. Treusch, N. Guerassimova, J. Feldhaus, C. Gutt, G. Grubel, S. Eisebitt, A. Beyer, A. Golzhauser, E. Weckert, M. Grunze, I. A. Vartanyants, and A. Rosenhahn, "X-ray holographic microscopy with zone plates applied to biological samples in the water window using 3rd harmonic radiation from the free-electron laser FLASH", Optics Express 19, Issue 12, pp.11059-11070 (2011).

[6] S. Roling, B. Siemer, M. Wostmann, H. Zacharias, R. Mitzner, A. Singer, K. Tiedtke, and I.A. Vartanyants, “Temporal and spatial coherence properties of free-electron-laser pulses in the extreme ultraviolet regime”, Phys. Rev. STAB 14, 080701/1-11 (2011).

[7] V. Hájková, L. Juha, P. Boháček, T. Burian, J. Chalupský, L. Vyšin, J. Gaudin, P.A. Heimann, S.P. Hau-Riege, M. M. Jurek, D. Klinger, J. Pelka, R. Sobierajski, J. Krzywinski, M.Messerschmidt, S.P. Moeller, B. Nagler, M. Rowen, W.F. Schlotter, M.L. Swiggers, J.J. Turner, S.M. Vinko, T. Whitcher, J. Wark, M. Matuchová, S. Bajt, H. Chapman, T. Dzelzainis, D. Riley, J. Andreasson, J. Hajdu, B. Iwan, N. Timneanu, K. Saksl, R. Fäustlin, A. Singer, K. Tiedtke, S. Toleikis, I. Vartaniants, H. Wabnitz, “X-ray laser-induced ablation of lead compounds”, Damage to VUV, EUV, and X-ray Optics III, edited by Libor Juha, Saša Bajt, Richard A. London, Proc. of SPIE, vol. 8077, 807718/1-7 (2011).

[8] A. Singer, and I.A. Vartanyants, “Modelling of partially coherent radiation based on the coherent mode decomposition”, Advances in Computational Methods for X-Ray Optics II, edited by Manuel Sanchez del Rio, Oleg Chubar, Proc. of SPIE, vol. 8141, 8141 06/1-9 (2011).

[9] J. Gulden, O.M. Yefanov, E. Weckert, and I.A. Vartanyants, “Imaging of Nanocrystals with Atomic Resolution Using High-Energy Coherent X-rays”, The 10th International Conference on X-ray Microscopy, AIP Conf. Proc. 1365, 42-45 (2011).

[10] I.A. Vartanyants, A. Singer, A.P. Mancuso, O.M. Yefanov, A. Sakdinawat, Y. Liu, E. Bang, G.J. Williams, G. Cadenazzi, B. Abbey, H. Sinn, D. Attwood, K.A. Nugent, E. Weckert, T. Wang, D. Zhu, B. Wu, C. Graves, A. Scherz, J.J. Turner, W.F. Schlotter, M. Messerschmidt, J. Luning, Y. Acremann, P. Heimann, D.C. Mancini, V. Joshi, J. Krzywinski, R. Soufli, M. Fernandez-Perea, S. Hau-Riege, A.G. Peele, Y. Feng, O. Krupin, S. Moeller, and W. Wurth, “Coherence Properties of Individual Femtosecond Pulses of an X-Ray Free-Electron Laser”, Phys. Rev. Lett. 107, 144801/1-5 (2011).

[11] J. Gulden, S. O. Mariager, A. P. Mancuso, O. M. Yefanov, J. Baltser, P. Krogstrup, J. Patommel, M. Burghammer, R. Feidenhans'l, and I.A. Vartanyants, "Coherent X-ray nanodiffraction on single GaAs nanowires", Phys. Status Solidi A, 208(11), 2495 (2011).

[12] I.A. Vartanyants, "Coherence properties of femtosecond pulses of an x-ray free-electron laser. Marching photons" Photon science 2011. Highlights and HASYLAB Annual Report, pp. 54-55 (DESY, Hamburg, 2012).

[13] J. Gulden, O.M. Yefanov, A.P. Mancuso, R. Dronyak, A. Singer, V. Bernátová, A. Burkhardt, O. Polozhentsev, A. Soldatov, M. Sprung, and I.A. Vartanyants, "Three-dimensional structure of a single colloidal crystal grain studied by coherent x-ray diffraction", Optics Express, 20(4), 4039 (2012).

[14] W.F. Schlotter, J.J. Turner, M. Rowen, P. Heimann, M. Holmes, O. Krupin, M. Messerschmidt, S. Moeller, J. Krzywinski, R. Soufli, M. Fernández-Perea, N. Kelez, S. Lee, R. Coffee, G. Hays, M. Beye, N. Gerken, F. Sorgenfrei, S. Hau-Riege, L. Juha, J. Chalupsky, V. Hajkova, A. P. Mancuso, A. Singer, O. Yefanov, I. A. Vartanyants, G. Cadenazzi, B. Abbey, K. A. Nugent, H. Sinn, J. Lüning, S. Schaffert, S. Eisebitt, W.-S. Lee, A. Scherz, A.R. Nilsson, and W. Wurth, "The soft x-ray instrument for material studies at the linac coherent light source x-ray free-electron laser", Rev. Sci. Instrum., 83, 043107 (2012).

[15] R.P. Kurta, M. Altarelli, E. Weckert and I. A. Vartanyants, "X-ray cross-correlation analysis applied to disordered two-dimensional systems", Phys. Rev. B (2012) in print.